Multiple Hydrogen Bond Interactions in the Processing of Functionalized Multi-Walled Carbon Nanotubes

Mildred Quintana,[†] Hassan Traboulsi,[‡] Anna Llanes-Pallas,[†] Riccardo Marega,[‡] Davide Bonifazi,[†,‡,*] and Maurizio Prato[†,*]

[†]Center of Excellence for Nanostructured Materials (CENMAT), INSTM UdR di Trieste, Dipartimento di Scienze Chimiche e Farmaceutiche, University of Trieste, Piazzale Europa 1, I-34127 Trieste, Italy, and [‡]Department of Chemistry, University of Namur (FUNDP), 5000 Namur, Belgium

ABSTRACT In a set of unprecedented experiments combining "bottom-up" and "top-down" approaches, we report the engineering of patterned surfaces in which functionalized MWCNTs have been selectively adsorbed on polymeric matrices as obtained by microlithographic photo-cross-linking of polystyrene polymers bearing 2,6-di(acetylamino)-4-pyridyl moieties (PS1) deposited on glass or Si. All patterned surfaces have been characterized by optical, fluorescence, and SEM imaging techniques, showing the local confinement of the CNTs materials on the polymeric microgrids. These results open new possibilities toward the controlled manipulation of CNTs on surfaces, using H-bonding self-assembly as the main driving force.

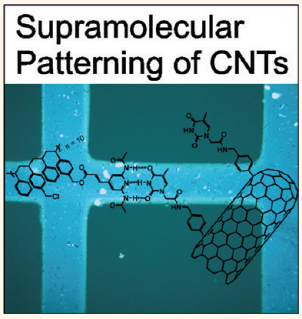

KEYWORDS: carbon nanotubes · functionalization · hydrogen bond · self-assembly · patterned surfaces · polymeric matrices

Organic-based materials help engineer matter at its molecular level, resulting in advanced applications with novel and significantly improved physical, chemical, and biological properties.[1−4] In nanotechnology, organic chemistry approaches can, in principle, provide alternative and valid solutions in electronics, optoelectronics, photonics, energy storage, and medicine.[5−7] Virtually, most of these technologies (from optics to electronics and sensors) rely on the interplay between the spatial molecular organization and the electronic motions, thus attaining the resolution and responsiveness necessary for practical applications. Therefore, the ability to organize in a controllable way individual or a small number of functional molecules or nano-objects on multidimensional scales is the key aspect in this engineering methodology.[8,9]

In this respect, CNTs are among the most studied materials for biology,[10−12] biosensors,[13−15] drug delivery,[16,17] transistors,[18,19] conductive layers,[20,21] field emitters,[22−24] and photovoltaics.[25,26] However, an unsettled issue pertinent to the construction of such CNT-based materials for nanotechnological applications is their precise localization and controllable spatial organization. As a result, the development of new protocols for patterning CNTs on substrates has become increasingly important for the fabrication of CNT-based devices.[27−29] Although several approaches have been developed for organizing CNTs on surfaces during their growth,[30,31] methods for post-growth organizations are awkward, often restricted to a narrow range of size scales compatible with nano- and microscopic patterning.[32,33] The conventional top-down lithographic methods, based on multiple preparative steps—resist patterning, etching, washing, and deposition—continue to be the industrial fabrication standard; however, integrating these methods with the recently developed protocol proper to the "bottom-up" strategies could offer preparative and operational advantages.[34,35] In terms of controlled organization, the self-assembly approach provides an extremely unique route toward the preparation of organized organic-based architectures patterned on surfaces.[36−39] In practical terms, this involves the preparation of preprogrammed molecular modules that, through specific functions, interact with themselves or with complementary units undergoing a defined hierarchical organization.[40,41] Among a myriad of examples displaying ordered structures at the nano and microscopic level, this strategy has been successfully used for patterning surfaces with functional molecular modules through the self-assembly of discrete, molecular-scale, H-bond assemblies,[42,43] as well as for the construction of very regular conductive nanoparticle films.[44] However, the

* Address correspondence to davide.bonifazi@fundp.ac.be; prato@units.it.

Received for review September 8, 2011 and accepted December 26, 2011.

Published online December 26, 2011
10.1021/nn203471t

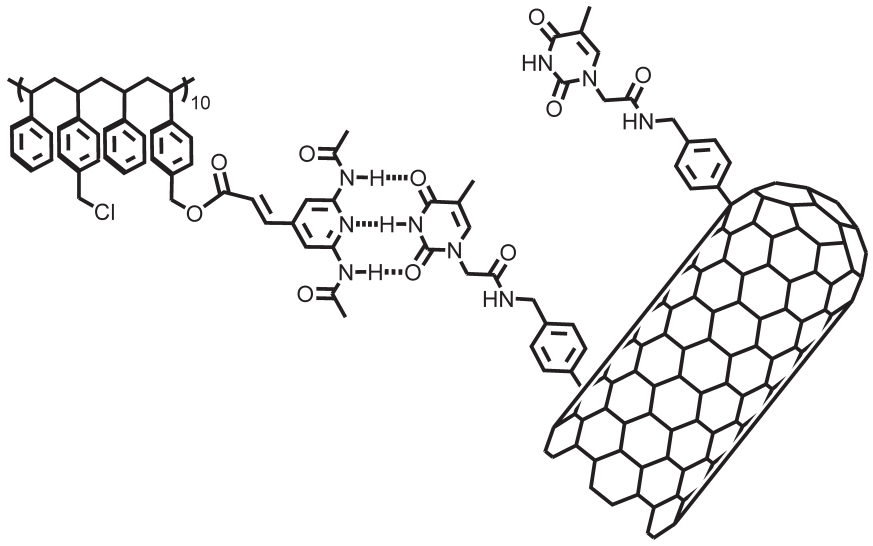

Scheme 1. Chemical structure of the supramolecular polymer−MWCNT hybrid complex, PS1·Thy-MWCNT.

preparative protocols for creating supramolecularly hierarchized architectures containing CNTs are severely hindered by their insolubility in most organic or aqueous solvents and their inherent low functionalization reproducibility. In this respect, the recent developments of efficient methodologies[45−47] for the chemical modification of CNTs have boosted the preparation of soluble and purified materials suitable for a given application.[48−51] Typically, two families of functionalization strategies are employed as chemical modification routes: a supramolecular and a covalent approach. Whereas the first protocol is based on the noncovalent coating of CNTs, conversely the second route exploits the chemical reactivity of the CNT graphitic wall by grafting organic chemical groups directly onto the tubular surface.[45,46] Among the macromolecular structures, polymers were revealed to be efficient noncovalent modifiers because of their extended chain-like structures, which, while wrapping around CNTs, can completely disrupt the van der Waals interactions within the nanotube bundles, improving their solubility and thus processability.[52−70] Recently, we have focused our attention on H-bonding interactions as directional, reliable, and predictable noncovalent attractive forces between complementary H-donor (D) and H-acceptor (A) moieties to control the self-organization process.[71−73] In this respect, we have recently reported one of the first examples of a molecular-recognition-driven assembly of CNTs in which newly designed thymine-derived CNTs (**Thy-CNTs**) self-organize in different solvents through the formation of double H-bonded homodimers, each composed of two modified thymine units covalently linked to the CNT surface.[74] As a practical development of our investigations, in this paper we report a simple methodology for the preparation of hybrid self-organized architectures in which CNTs are locally organized on patterned surfaces coated with a polymeric matrix. Specifically, the protocol involves the self-assembly of thymine-functionalized MWCNTs (**Thy-MWCNTs**) with polystyrene polymers bearing 2,6-di(acetylamino)-4-pyridyl moieties (**PS1**) through triple complementary ADA-DAD H-bonding interactions (**PS1·Thy-MWCNTs**, Scheme 1). The supramolecular **PS1·Thy-MWCNT** complexes were characterized by absorption and fluorescence spectroscopy, transmission electron microscopy (TEM), atomic force microscopy (AFM), and thermogravimetric analysis (TGA), which taken together, proved the formation of H-bond-driven supramolecular complexes **PS1·Thy-MWCNTs**. Through a combination of a "top-down" and a "bottom-up" methodology, we successively prepared patterned surfaces with CNTs. Optical fluorescence and scanning electron microscopy (SEM) displayed the selective surface confinement of the CNT material.

RESULTS AND DISCUSSION

As depicted in Scheme 1, the engineering design behind the formation of the supramolecular CNT−polymer complex is the establishment of three H-bonds between the complementary sites of the di(acetylamino)pyridine group (DAD) and the thymine (ADA) moieties covalently attached to the polystyrene and MWCNTs, respectively. Di(acetylamino)pyridine-bearing polystyrene **PS1** was prepared *via* radical polymerization of styrene with 4-chloromethylstyrene in the presence of AIBN followed by reaction of the precursor polymer co-PSCl with 2,6-di(acetylamino)-4-pyridylacrylic acid as described in the Experimental Part (see Scheme 1, SI). Conversion was determined estimating the peak area between the proton resonance centered at 7.9 ppm belonging to the pyridyl and the proton resonance region between 6 and 7.6 ppm corresponding to the aromatic groups (SI-1). Specifically, a 50% conversion of the $-CH_2Cl$ functionality

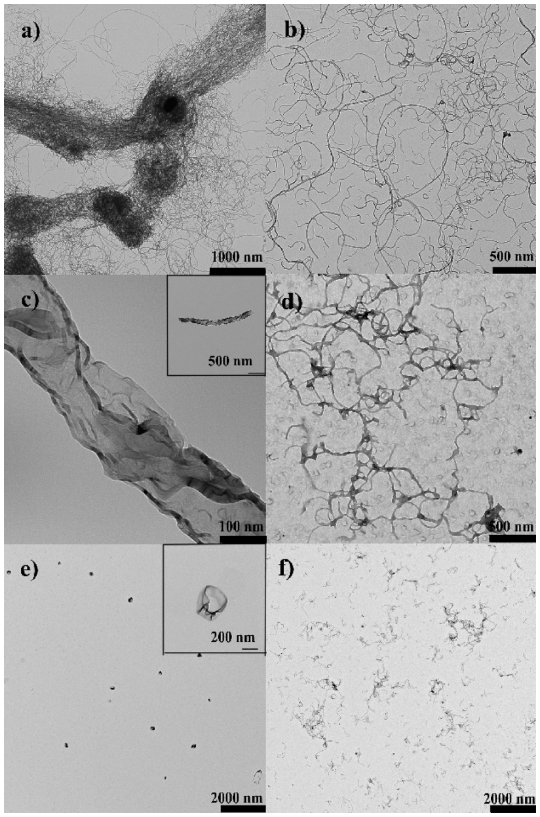

Figure 1. TEM micrographs of Thy-MWCNTs in (a) $CHCl_3$ and (b) DMF; (c) PS1·Thy-MWCNTs in $CHCl_3$, ([PS1] = 0.05 mg mL^{-1} and [Thy-MWCNTs] = 0.02 mg mL^{-1}); (d) PS1/Thy-MWCNTs ([PS1] = 0.05 mg mL^{-1} and [Thy-MWCNTs] = 0.02 mg mL^{-1}) in DMF; (e) PS1·Thy-MWCNTs in $CHCl_3$ ([PS1] = 1×10^{-6} mg mL^{-1} and [Thy-MWCNTs] = 3.5×10^{-8} mg mL^{-1}); (f) PS1/Thy-MWCNTs ([PS1] = 1×10^{-6} mg mL^{-1} and [Thy-MWCNTs] = 3.5×10^{-8} mg mL^{-1}) in DMF.

has been found, showing a good conversion of the esterification reaction. An average M_w of 4650 Da and PD = 1.49 were determined by gel permeation chromatography (GPC). IR spectra, shown in SI-2, also confirmed the presence of the complementary 2,6-di(acetylamino)-4-pyridyl (DAD) recognition functions within the polymer resin through the characteristic amidic and steric CO-centered stretching vibration at 1640 and 1750 cm^{-1}, respectively. **Thy-MWCNTs** were prepared by addition of the diazonium derivative of 4-Boc-aminomethylaniline to MWCNTs, followed by acid cleavage (with 4 M HCl aqueous solution) of the BOC protecting group. The amide-bond formation reaction was then achieved between the free amino groups present in the amino-CNTs and the carboxylic functionalities of the thymine derivatives.[75] Taken all together, quantitative Kaiser test, XPS analysis, TGA, and TGA-MS, along with the different observed dispersibility behavior of pristine MWCNTs7000 compared to that of the functionalized **Thy-MWCNTs** in an appropriate organic solvent, proved the covalent attachment of the functional groups (SI-3−SI-6). In particular, the quantification of the free amino groups before and after the amidation reaction[76] gives the final loading of thymine molecules attached to MWCNTs, which resulted in an average value of 765 μmol g^{-1}. These results revealed to be in good agreement with the XPS findings obtained for **Thy-MWCNTs** samples (SI-4). The spectrum survey reveals the presence of the resonance peaks from C 1s (284.7 eV), N 1s (400 eV), and O 1s (533.1 eV). The presence of N 1s ($2 \pm 0.4\%$) in the elemental composition indicates that the MWCNTs have been efficiently functionalized with N-containing thymine moieties since N is not present in the elemental composition of the pristine MWCNTs.

The complexation behavior between **PS1** and **Thy-MWCNTs** has been first analyzed by TEM and AFM. Although it is known that the association between molecular modules bearing multiple H-bonding units depends on the number and on the relative spatial arrangement of neighboring H-donor and H-acceptor sites, this process is largely influenced by the medium (solvent, temperature, and pressure). For uracyldi-(acetylamino)pyridine heterodimers typical values of K_a in $CHCl_3$ amount to $\sim 10^3$.[77−80] Hence, the recognition between **PS1** and **Thy-MWCNTs** was studied in different solvents, such as $CHCl_3$ and in DMF at different temperatures. As recently reported,[74] functionalized CNTs **Thy-MWCNTs** aggregate in noncompetitive solvents such as $CHCl_3$ (Figure 1a), whereas good dispersions can be obtained in DMF (Figure 1b). Noteworthy, when a mixture of **PS1** and **Thy-MWCNTs** was suspended in $CHCl_3$, stable dispersions at diluted concentrations were obtained ([**PS1**] = 1×10^{-6} mg mL^{-1} and [**Thy-MWCNTs**] = 3.5×10^{-8} mg mL^{-1}). In particular, the presence of polymer **PS1** leads to the selective formation of supramolecular aggregates (**PS1·Thy-MWCNTs**) in which the thymine-functionalized carbon nanotubes **Thy-MWCNTs** are in intimate contact with the polymeric counterpart through the complementary triple ADA-DAD H-bonding interactions. This induces a wrapping of the polymer around the CNT walls and thus disaggregation of the CNT bundles, improving their solubility in other organic solvents such as $CHCl_3$.

TEM micrographs of drop-cast solutions of **PS1·Thy-MWCNTs** in $CHCl_3$ at the millimolar level ([**PS1**] = 0.05 mg mL^{-1} and [**Thy-MWCNTs**] = 0.02 mg mL^{-1}) show the appearance of tubular structures (~200 and 1000 nm, diameter and length, respectively, Figure 1c), in which single CNTs are wrapped by the polymer. Notably, at the micromolar level ([**PS1**] = 1×0^{-6} mg mL^{-1} and [**Thy-MWCNTs**] = 3.5×10^{-8} mg mL^{-1}), **PS1·Thy-MWCNTs** form small semispherical aggregates (~350 nm in diameter, Figure 1e). As expected, the triple ADA-DAD H-bonding interactions between the complementary thymine and diacetylamidopyridyl units drive the formation of **PS1·Thy-MWCNT** hybrid complexes in $CHCl_3$, consequently avoiding the self-aggregation of **Thy-MWCNT** derivatives in which only the double H-bonds of the thymine-based pairs are established. At the same time, increasing the

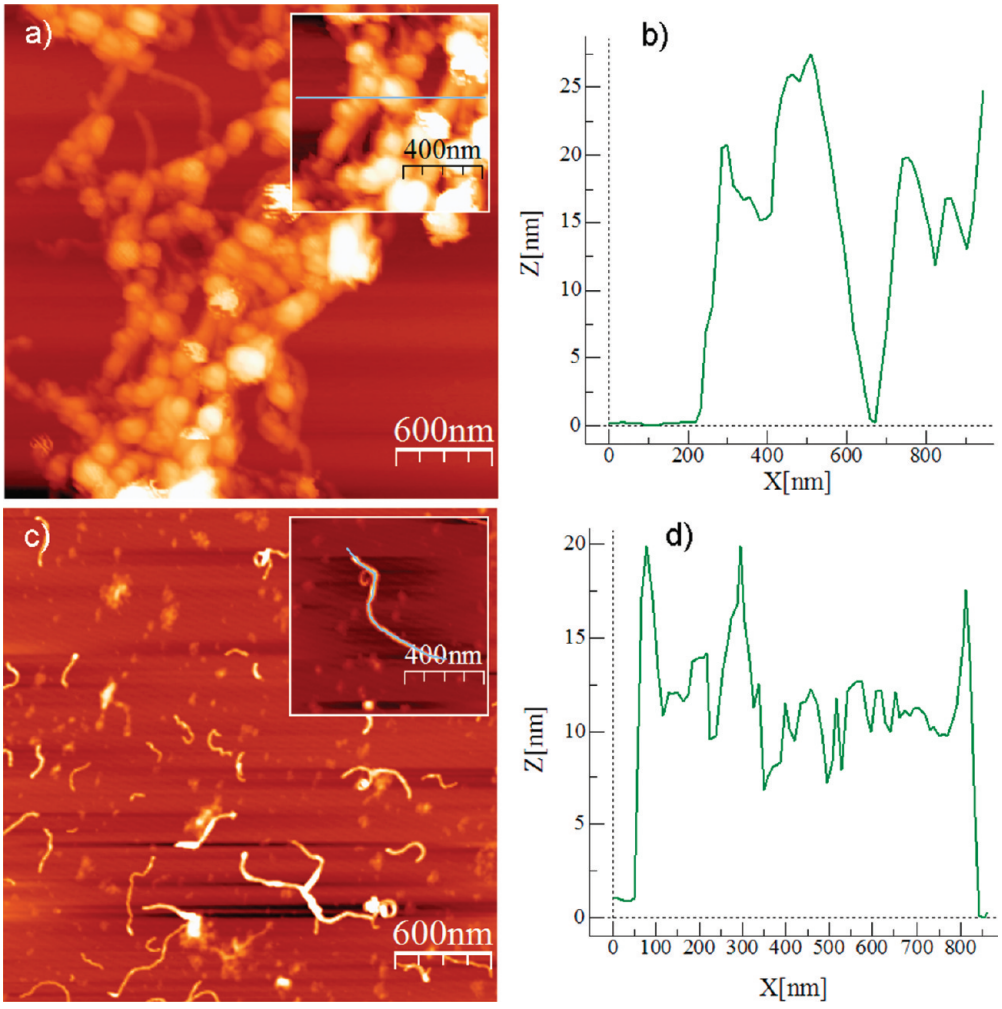

Figure 2. AFM topography obtained on mica from drop-cast dispersions ([PS1] = 0.05 mg mL^{-1} and [Thy-MWCNTs] = 0.02 mg mL^{-1}) of PS1·Thy-MWCNTs in (a) $CHCl_3$ and (c) DMF; (b and d) HR-AFM cross-section profiles of the insets .

concentration of the dispersions (PS1 + Thy-MWCNTs) mixtures leads to the progressive assembly of larger supramolecular entities. The process involves the growth of tridimensional aggregates from semi-spherical to tubular ones. TEM studies of the mixtures of **PS1** and **Thy-MWNTs** deposited from DMF dispersions were also carried out as control experiments. No evidence of supramolecular **PS1·Thy-MWCNTs** complexes were obtained, and only mixtures of free polymer **PS1** and individual **Thy-MWCNTs** nanotubes could be observed (Figure 1d and f). This is attributed to a solvent effect, as DMF competes with the H-bonding formation, preventing the recognition between **PS1** and **Thy-MWCNTs** in solution, thus leading to segregation effects once the solutions are deposited on the surface. TEM investigations using physical mixtures containing **PSCl** polymer (*i.e.*, without the 2,6-di(acetylamino)pyridyl functionalities) or pristine **MWCNTs** have also been carried out (see Figures SI-7 and SI-8). As expected, in both cases no supramolecular complexes were formed and only inhomogeneous mixtures of the separated components have been observed, indirectly proving the effectiveness of the H-bonding-driven recognition between **PS1** and **Thy-MWCNTs** in hybrid **PS1·Thy-MWCNTs**.

Tapping-mode AFM analysis was also used to characterize the morphology of the supramolecular complexes **PS1-Thy·MWCNTs** as formed in $CHCl_3$ dispersions. Figure 2 shows typical AFM images obtained for **PS1** and **Thy-MWCNTs** ([**PS1**] = 0.05 mg mL^{-1} and [**Thy-MWCNTs**] = 0.02 mg mL^{-1}) mixtures, where Figure 2a corresponds to the supramolecular system **PS1-Thy·MWCNTs** as obtained from $CHCl_3$, while Figure 2c shows a mixture containing non-bonded **PS1** and **Thy-MWCNTs** as obtained from DMF. High-resolution AFM height profiles of the insets are shown in Figure 2b and d. As produced, pristine MWCNTs have an average diameter of 9.5 nm.[81] HR-AFM profiles indicate that **PS1** approximately coats the entire exosurface of **Thy-MWCNTs** in Figure 2b, whereas in Figure 2c only a few areas of the tube external wall are covered by **PS1**.

Since the absorption and emission properties of the polymer can be strongly influenced by its complexation

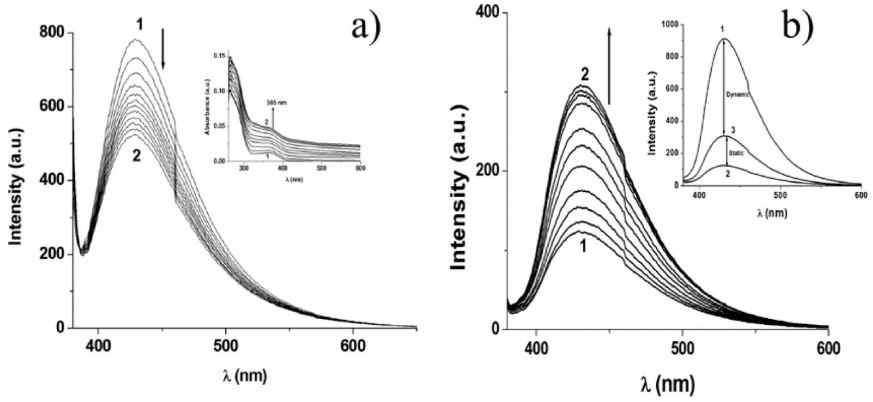

Figure 3. (a) Spectrofluorimetric titration of PS1 by Thy-MWCNTs. Solvent = 1,1,2,2, $C_2H_2Cl_4$; [PS1] = 1.3 × 10^{-2} mg mL^{-1}; (1) [Thy-MWCNTs] = 0.0; (2) [Thy-MWCNTs] = 1.5 × 10^{-3} mg mL^{-1}. (b) Spectrofluorimetric titration of hybrid PS1·Thy-MWCNTs upon addition of increasing volumes (*V*) of DMSO ([PS1] = 2.0 × 10^{-2} mg mL^{-1}; [Thy-MWCNTs] = 1.9 × 10^{-2} mg mL^{-1}; (1) V_{DMSO} = 0 mL and (2) V_{DMSO} = 56 mL). Inset: Emission spectra displaying the radiative emission in the static and dynamic quenching regime: (1) only PS1; (2) assembly PS1·Thy-MWCNTs; (3) after addition of 56 mL of DMSO. Solvent = TCE.

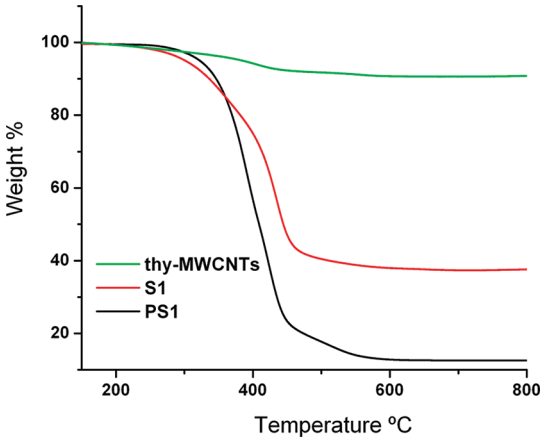

Figure 4. TGA performed under nitrogen of PS1 (black), Thy-MWCNTs (green), and PS1·Thy-MWCNTs (red) as prepared in $CHCl_3$.

with the CNT conjugate, we have investigated the association properties by means of steady-state UV–vis–NIR absorption and fluorescence spectroscopy (SI-9–SI-11). UV–vis–NIR absorption and spectrofluorimetric titrations of a solution of **PS1·Thy-MWCNTs** in 1,1′,2,2′-$C_2H_2Cl_4$ (TCE) upon addition of DMSO (Figure 3) show that upon increasing concentrations of DMSO, the polymer-centered emission intensity progressively increases, giving a clear indication of the expected assembly dissociation as a consequence of the presence of the DMSO solvent molecules disrupting the H-bonding interactions. Conversely, UV–vis–NIR titration spectra show an extended decrease of the band intensity upon increasing concentrations of DMSO. This observation could be explained by the reduced dispersibility of the **Thy-MWCNTs** in DMSO that, competing with ADA–DAD H-bonding interactions, prevents the formation of the hybrid complex **PS1·Thy-MWCNTs**, thus inducing precipitation of the carbon material. In order to examine the thermal stability of the H-bonded **PS1·Thy-MWCNTs** complex, variable-temperature (VT) UV–vis measurements were also carried out (Figures SI-10 and SI-11). A reversible thermal behavior (*i.e.*, from 90 to 25 °C) was observed. In particular, the intensity of the absorption spectrum decreases with the increase of the temperature (from room temperature to 90 °C). This is a completely reversible process, as increasing intensity absorptions can be observed upon thermal cooling (to 25 °C). Reference VT UV–vis absorption measurements were also performed with solutions containing only **Thy-MWCNTs**, displaying a similar absorbance behavior to that observed for **PS1·Thy-MWCNTs**, suggesting a CNT-controlled thermal process.

The amount of **PS1** attached to **Thy-MWCNTs** was estimated by TGA measurements (Figure 4). At first, **PS1** was copiously washed by filtration with $CHCl_3$ until no UV–vis absorption signal of **PS1** was noticeable in the filtered solution. Then, the precipitate was dried overnight under vacuum. The temperature-modulated plot of polymer **PS1** shows a steep weight loss in the range 100 to 600 °C, with a residual weight at 600 °C close to 10% w/w (Figure 4). The complex **PS1·Thy-MWCNTs** show an analogous weight loss of approximately 60% w/w at 600 °C, whereas the **Thy-MWCNTs** loss is limited to approximately 10% w/w at the same temperature. This result clearly indicates that the **PS1·Thy-MWCNTs** moiety in **PS1** is *ca.* 50% w/w. Notably, this observation is in very good agreement with TEM (Figures 1b,c) and spectroscopic characterizations, further supporting the evidence for which polymer **PS1** selectively wraps **Thy-MWCNTs** forming the hybrid aggregates.

Using the recognition properties between the polymer and **Thy-MWCNTs**, we were able to prepare CNT-containing patterned surfaces (on glass or Si). Surface modification was conducted in a stepwise approach, exploiting both a lithographic method ("top-down") and the complementary H-bonding interactions between **Thy-MWCNTs** and polymer **PS1** ("bottom-up"). A solution

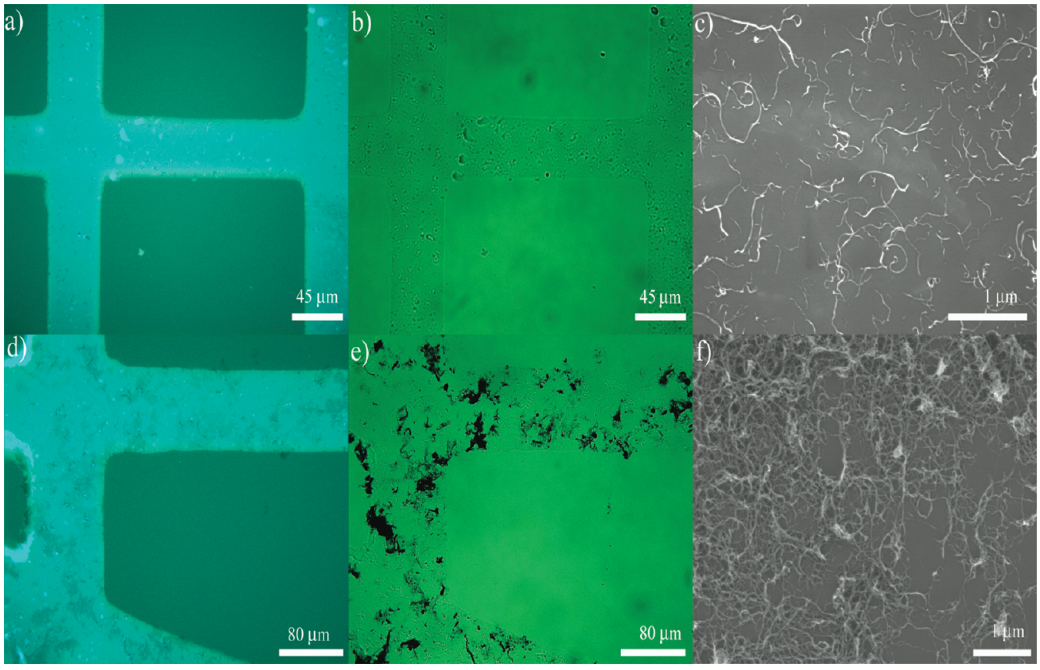

Figure 5. Imaging of the patterned surfaces by (a, d) fluorescence (10×), (b, e) optical (10×), and (c, f) SEM microscopy after the deposition of a dispersion of Thy-MWCNTs in DMF (a–c) and $CHCl_3$ (d–f).

of polymer **PS1** (10 mg mL^{-1} in DMF or $CHCl_3$) was first spin-coated on clean surfaces, leading to homogeneous thin films. Stabilization of the films by photo-cross-linking under a photoresist mask[82] followed by copious rinsing with DMF (or $CHCl_3$), to remove the unlinked polymer, led to the patterned surface shown in Figure 5. The films revealed to be particularly stable upon treatment with MeOH, C_2H_4O, or H_2O. Selective deposition of the CNT materials was accomplished by dipping the patterned **PS1**-coated surfaces into a dispersion of **Thy-MWCNTs** (0.5 mg mL^{-1}) in DMF (Figures 5a–c) or $CHCl_3$ (Figures 5d–f) for two hours, followed by repetitive washing and drying cycles. Directed by the complementary triple ADA–DAD H-bonding interactions, functionalized **Thy-MWCNTs** were confined only on those surface regions actually covered by photo-cross-linked polymer **PS1**. This was confirmed by fluorescence microscopic imaging measurements, which clearly show a monolayer of adsorbed **Thy-MWCNTs** from DMF only on the irregular regions of the polymeric patterned grids (Figure 5b; only **PS1**-patterned surfaces are shown in Figure 5a). SEM micrographs (Figure 5c) corroborated the presence of **Thy-MWCNTs** regularly distributed on the patterned surface. It was also noticed that, increasing the concentration of the **Thy-MWCNTs** dispersion, the monolayer coverage increased (SI-12). Surprisingly, despite the higher H-bonding competitiveness of DMF with respect to $CHCl_3$, higher and homogeneous coverage was obtained with dispersions of **Thy-MWCNTs** in DMF (Figure 5a–c). Conversely, deposition from $CHCl_3$ dispersions produced inhomogeneous surfaces in which aggregated **Thy-MWCNTs** material was adsorbed on the patterned polymer (Figure 5d–f). At a first view, this observation can be contradictory. However, this is attributed to the better dispersibility of **Thy-MWCNTs** in DMF, as homomolecular double H-bonding Thy–Thy interactions are weaker in such a solvent. Nevertheless, it is interesting to note that upon evacuation of the organic solvents, the deposited **Thy-MWCNTs** displayed unprecedented stability, being resistant to further washing cycles. Reference experiments, in which polymer **PS1** has been replaced with **PSCl** (see Experimental Part), were performed in order to demonstrate the effectiveness of the complementary H-bonding interactions for the controlled adsorption of functionalized CNTs. As expected, SEM imaging indicated the absence of **Thy-MWCNTs** on the patterned **PSCl** polymer after identical treatment. Similar results have been also obtained when a dispersion of pristine MWCNTs were deposited on **PS1**-containing patterned surfaces, demonstrating the need for the thymine moieties on the CNTs' exosurface to locally confine the carbon materials on the polymeric layer (SI-13).

In conclusion, by means of directional triple heteromolecular H-bonding interactions, it was possible to prepare stable CNT–polymer hybrids following a self-assembly approach. The recognition between the components is driven by the establishment of triple complementary H-bonds between the di(acetylamino) pyridine and thymine moieties, respectively appended on the polymer and on the MWCNTs' external carbon wall. Microscopic and spectroscopic techniques unambiguously confirmed the formation of the hybrid **PS1**·**Thy-MWCNTs** complexes, as obtained from apolar noncompetitive solvents such as $CHCl_3$ or TCE. Spectroscopic results proved that the supramolecular recognition between these two components occurs *via*

the H-bonding recognition, as no hybrid **PS1-MWCNT** complexes formed from the dispersion mixtures of pristine MWCNTs and the polymers. In a set of unprecedented experiments combining "bottom-up" and "top-down" approaches, we have also engineered the first patterned surfaces in which functionalized MWCNTs have been selectively adsorbed on patterned surfaces as obtained by microlithographic photo-cross-linking of **PS1** deposited on glass or Si. All patterned surfaces have been characterized by optical, fluorescence, and SEM imaging techniques, showing the local confinement and deposition of the CNT materials on the specifically designed polymeric microgrids. The quality of the produced **Thy-MWCNTs** monolayer patterns basically depends on the polymer photo-cross-linking resolution[82] and the concentration of the **Thy-MWCNTs** dispersion. These results are of significant importance since they open new possibilities toward the controlled manipulation of CNTs for the engineering of CNT-based electronic devices or biomaterials. For instance, merging the "top-down" and the "bottom-up" approaches, it can be envisaged to controllably organize and manipulate biocompatible functionalized CNTs on various substrates for producing bioactive surfaces for the directed growth of neuronal cells on patterned surfaces.[83]

Acknowledgment. This work was supported by the Italian Ministry of Education MIUR (cofin Prot. 20085M27SS), the European Union through the ERC Advanced Grant Carbonanobridge (contract ERC ADG 2008 - Grant Agreement 227135), Marie-Curie Research Training Network "PRAIRIES" (contract MRTN-CT-2006-035810), the Marie-Curie Initial Training Network "FINELUMEN" (grant agreement PITN-GA-2008-215399), INSTM, the Belgian National Research Foundation (through the FRFC contract nos. 2.4.625.08, 2.4.550.09, and 2.4.617.07.F and the MIS no. F.4.505.10.F), the "Loterie Nationale", the Région Wallonne through the "SOLWATT" program (contract no. 850551), the "TINTIN" ARC project from the Belgian French Community (contract no. 09/14-023), and the University of Namur and University of Trieste. H.T. thanks the FUNDP's institutional CERUNA program and the FNRS-FSR for his postdoctoral fellowships. R.M. thanks the FNRS-FSR for his postdoctoral fellowship. We thank Dr. Francesca Maria Toma for help with the SEM characterizations, Prof. Luisa Schenetti (University of Modena) and Dr. Massimiliano Lanzi (Dipartimento di Chimica Industriale e dei Materiali, University of Bologna) for GPC measurements, Dr. Luigi Feruglio for help with NMR analysis, and Mr. Claudio Gamboz for the assistance with the TEM characterizations.

Supporting Information Available: Experimental section. SI-1: ^{1}H NMR of **PS1**. SI-2: IR spectra of 2,6-di(acetylamino)-4-pyridylacrylic acid and **PS1**. SI-3: TGA presenting the different functionalization steps during the synthesis of **Thy-MWCNTs**. SI-4: XPS analysis of **Thy-MWCNTs.** SI-5: TGA-MS analysis of **Thy-MWCNTs**. SI-6: Dispersibility test of **Thy-MWCNTs**. SI-7 and SI-8: TEM micrographs of control experiments. SI-9 to SI-11: UV−vis absorption and fluorescence titrations. This material is available free of charge *via* the Internet at http://pubs.acs.org.

REFERENCES AND NOTES

1. Kneipp, K.; Kneipp, H.; Dasari, I.; Feld, R. R.; Feld, M. S. Surface-Enhanced Raman Scattering and Biophysics. *J. Phys. Condens. Matter* **2002**, *14*, R597–R624.
2. Auletta, T.; Dordi, B.; Mulder, A.; Sartori, A.; Onclin, S.; Bruinink, C. M.; Peter, M.; Nijhuis, C. A.; Beijleveld, H.; Schonherr, H.; *et al.* Writing Patterns of Molecules on Molecular Printboards. *Angew. Chem., Int. Ed.* **2004**, *43*, 369–373.
3. Xia, Y.; Halas, N. J. Shape-Controlled Synthesis and Surface Plasmonic Properties of Metallic Nanostructures. *MRS Bull.* **2005**, *30*, 338–348.
4. Barnes, W. L.; Dereux, A.; Ebbesen, T. W. Reticular Synthesis and the Design of New Materials. *Nature* **2003**, *30*, 338–348.
5. Yaghi, O. M.; O'Keeffe, M.; Ockwing, N. W.; Chae, H. K.; Eddaoudi, M.; Kim, J. Higher-Order Organization by Mesoscale Self-Assembly and Transformation of Hybrid Nanostructures. *Nature* **2003**, *423*, 705–714.
6. Colfen, H.; Mann, S. Nanofabrication with Elastomeric Molds and Stamps. *Angew. Chem., Int. Ed.* **2003**, *42*, 2350–2365.
7. Gates, B. D.; Xu, Q.; Stewar, M.; Ryan, D.; Willson, C. G.; Whitesides, G. M. New Approaches to Nanofabrication: Molding, Printing, and Other Techniques. *Chem. Rev.* **2005**, 1171–1196.
8. Reed, M. A.; Zhou, C.; Muller, C. J.; Burgin, T. P.; Tour, J. M. Conductance of a Molecular Junction. *Science* **1997**, *278*, 252–254.
9. Postma, H. W. C.; Teepen, T.; Yao, Z.; Grifoni, M.; Dekker, C. Carbon Nanotube Single-Electron Transistors at Room Temperature. *Science* **2001**, *293*, 76–79.
10. Zhang, X.; Prasad, S.; Niyogi, S.; Morgan, A.; Ozkan, M.; Ozkan, C. S. Hybrid Neurite Growth on Patterned Carbon Nanotube Substrates. *Sens. Actuators B* **2005**, *106*, 843–850.
11. Zhang, S. Fabrication of Novel Biomaterials Through Molecular Self-Assembly. *Nat. Biotechnol.* **2003**, *21*, 1171–1178.
12. Mazzatenta, A.; Giugliano, M.; Campidelli, S.; Gambazzi, L.; Businaro, L.; Markram, H.; Prato, M.; Ballerini, L. Interfacing Neurons with Carbon Nanotubes: Electrical Signal Transfer and Synaptic Stimulation in Cultured Brain Circuits. *J. Neurosci.* **2007**, *27*, 6931–6936.
13. Gruner, G. Carbon Nanotube Transistors for Biosensing Applications. *Anal. Bioanal. Chem.* **2006**, *384*, 322–335.
14. Balasubramanian, K.; Burghard, M. Biosensors Based on Carbon Nanotubes. *Anal. Bioanal. Chem.* **2006**, *385*, 452–468.
15. Timko, B. P.; Cohen-Karni, T.; Qing, Q.; Tian, B.; Lieber, C. M. Design and Implementation of Functional Nanoelectronic Interfaces with Biomolecules, Cells and Tissue Using Nanowire Device Arrays. *IEEE Trans. Nanotech.* **2010**, 269–280.
16. Bianco, A.; Kostarelos, K.; Prato, M. Making Carbon Nanotubes Biocompatible and Biodegradable. *Chem. Commun.* **2011**, *47*, 10182–10188.
17. Lacerda, L.; Bianco, A.; Prato, M.; Kostarelos, K. Carbon Nanotube Cell Translocation and Delivery of Nucleic Acids *in Vitro* and *in Vivo*. *J. Mater. Chem.* **2008**, *18*, 17–22.
18. Javey, A.; Guo, J.; Farmer, D. B.; Wang, Q.; Wang, D.; Gordon, R. G.; Lundstrom, M.; Dai, H. Carbon Nanotube Field-Effect Transistors with Integrated Ohmic Contacts and High-k Gate Dielectrics. *Nano Lett.* **2004**, *4*, 447–450.
19. Wu, Z.; Chen, Z.; Du, X.; Logan, J. M.; Sippel, J.; Nikolou, M.; Kamaras, K.; Reynolds, J. R.; Tanner, D. B.; Hebard, A. F.; *et al.* Transparent, Conductive Carbon Nanotube Films. *Science* **2004**, *305*, 1273–1276.
20. Esplandiu, M. J.; Bittner, V. G.; Giapis, K. P.; Collier, C. P. Nanoelectrode Scanning Probes from Fluorocarbon-Coated Single-Wall Carbon Nanotubes. *Nano Lett.* **2004**, *4*, 1873–1879.
21. Shim, B. S.; Tang, Z. Y.; Morabito, Z. M. P.; Agarwal, A.; Hong, H.; Kotov, N. A. Integration of Conductivity, Transparency, and Mechanical Strength into Highly Homogeneous Layer-by-Layer Composites of Single-Walled Carbon Nanotubes for Optoelectronics. *Chem. Mater.* **2007**, *19*, 5467–5474.
22. Jeong, H. J.; Choi, H. K.; Kim, G. Y.; Il Song, Y.; Tong, Y.; Lim, S. C.; Lee, Y. H. Fabrication of Efficient Field Emitters with Thin Multiwalled Carbon Nanotubes Using Spray Method. *Carbon* **2006**, *44*, 2689–2693.

23. Kumar, M; Okazaki; Hiramatsu, T. M.; Ando, Y. The Use of Camphor-Grown Carbon Nanotube Array as an Efficient Field Emitter. *Carbon* **2007**, *45*, 1899–1904.
24. Wei, W.; Liu, Y.; Wei, Y.; Jiang, K.; Peng, L.-M.; Fan, S. Tip Cooling Effect and Failure Mechanism of Field-Emitting Carbon Nanotubes. *Nano Lett.* **2007**, *7*, 64–68.
25. Campidelli, S.; Klumpp, C.; Bianco, A.; Guldi, D. M.; Prato, M. Functionalization of CNT: Synthesis and Applications in Photovoltaics and Biology. *J. Phys. Org. Chem.* **2006**, *19*, 531–539.
26. Guldi, D. M.; Rahman, G. M. A.; Zerbetto, F.; Prato, M. Carbon Nanotubes in Electron Donor−Acceptor Nanocomposites. *Acc. Chem. Res.* **2005**, *38*, 871–878.
27. Lee, S. W.; Yabuuchi, N.; Gallat, B. M.; Chen, S.; Kim, B.-S.; Hammond, P. T.; Shao-Horn, Y. High-Power Lithium Batteries from Functionalized Carbon Nanotube Electrodes. *Nat. Nanotechnol.* **2010**, *5*, 531–537.
28. Kotov, N. A.; Winter, J. O; Clements, I. P.; Jan, E.; Timko, B. P.; Campidelli, S.; Pathak, S.; Mazzatenta, A.; Lieber, C. M.; Prato, M. L.; *et al*. Nanomaterials for Neural Interfaces. *Adv. Mater.* **2009**, *21*, 3970–4004.
29. Terrones, M. Science and Technology of the Twenty-First Century: Synthesis, Properties, and Applications of Carbon Nanotubes. *Annu. Rev. Mater. Res.* **2003**, *33*, 419–501.
30. Wei, B. Q.; Vajtai, R.; Jung, Y.; Ward, J.; Zhang, R.; Ramanath, G.; Ajayan, P. M. Microfabrication Technology: Organized Assembly of Carbon Nanotubes. *Nature* **2002**, *416*, 495–496.
31. Zhang, J. Z.; Wei, B. Q.; Ramanath, G.; Ajayan, P. M. Substrate-Site Selective Growth of Aligned Carbon Nanotubes. *Appl. Phys. Lett.* **2000**, *77*, 3764–3768.
32. Diehl, M. R.; Yaliraki, S. N.; Beckman, R. A.; Barahona, M.; Heath, J. R. Self-Assembled, Deterministic Carbon Nanotube Wiring Networks. *Angew. Chem., Int. Ed.* **2002**, *41*, 353–356.
33. Smith, B. W.; Benes, Z.; Luzzi, D. E.; Fischer, J. E.; Walters, D. A.; Casavant, M. J.; Schmidt, J.; Smalley, R. E. Structural Anisotropy of Magnetically Aligned Single Wall Carbon Nanotube Films. *Appl. Phys. Lett.* **2000**, *77*, 663–665.
34. Lopes, W. A.; Jaeger, H. M. Hierarchical Self-Assembly of Metal Nanostructures on Diblock Copolymer Scaffolds. *Nature* **2001**, *414*, 735–738.
35. Freeman, R. G.; Grabar, K. C.; Allison, K. J.; Bright, R, M.; Davis, J. A.; Guthrie, A. P.; Hommer, M. B.; Jackson, M. A.; Smith, P. C.; Walter, D. G.; *et al*. Self-Assembled Metal Colloid Monolayers: An Approach to SERS Substrates. *Science* **1995**, *267*, 1629–1632.
36. Lehn, J. M. Perspectives in Supramolecular Chemistry—From Molecular Recognition towards Molecular Information Processing and Self-Organization. *Angew. Chem., Int. Ed. Engl.* **1990**, *29*, 1304–1319.
37. Whitesides, G. M.; Mathias, J. P.; Seto, C. T. Molecular Self-Assembly and Nanochemistry: A Chemical Strategy for the Synthesis of Nanostructures. *Science* **1991**, *254*, 1312–1319.
38. Whitesides, G. M. Self-Assembling Materials. *Sci. Am.* **1995**, *273*, 146–149.
39. Whitesides, G. M.; Grzybowski, B. A. Self-Assembly at All Scales. *Science* **2002**, *295*, 2418–2421.
40. Whitcombe, M. J.; Vulfson, E. V. Imprinted Polymers. *Adv. Mater.* **2001**, *12*, 467–478.
41. Maynor, B. W.; La Rue, I.; Hu, Z.; Spontak, J. P.; Sheiko, S. S.; Samulski, R. J.; Samulski, E. T.; De Simone, J. M. Supramolecular Nanomimetics: Replication of Micelles, Viruses, and Other Naturally Occurring Nanoscale Objects. *Small* **2007**, 845–849.
42. Llanes-Pallas, A.; Matena, M.; Jung, T.; Prato, M.; Stohr, M.; Bonifazi, D. Trimodular Engineering of Linear Supramolecular Miniatures on Ag(111) Surfaces Controlled by Complementary Triple Hydrogen Bonds. *Angew. Chem., Int. Ed.* **2008**, *47*, 7726–7730.
43. Llanes-Pallas, A.; Palma, C. A.; Piot, L.; Belbakra, A.; Listorti, A.; Prato, M.; Samorì, P.; Armaroli, N.; Bonifazi., D. Engineering of Supramolecular H-Bonded Nanopolygons *via* Self-Assembly of Programmed Molecular Modules. *J. Am. Chem. Soc.* **2009**, *131*, 509–520.
44. Xu, H.; Hong, R.; Wang, X.; Arvizo, R.; You, C.; Samanta, B.; Patra, D.; Tuominen, M. T.; Rotello, V. M. Controlled Formation of Patterned Gold Films *via* Site-Selective Deposition of Nanoparticles onto Polymer Templated Surfaces. *Adv. Mater.* **2007**, *19*, 1383–1386.
45. Singh, P.; Campidelli, S.; Giordani, S.; Bonifazi, D.; Bianco, A.; Prato, M. Organic Functionalisation and Characterisation of Single-Walled Carbon Nanotubes. *Chem. Soc. Rev.* **2009**, *38*, 2214–2230.
46. Tasis, D.; Tagmatarchis, N.; Bianco, A.; Prato, M. Chemistry of Carbon Nanotubes. *Chem. Rev.* **2006**, *106*, 1105–1136.
47. Start, A.; Steuerman, D. W.; Heath, J. R.; Stoddart, J. F. Starched Carbon Nanotubes. *Angew. Chem., Int. Ed.* **2002**, *41*, 2508–2512.
48. Jan, E.; Hendricks, J. L.; Huasini, V.; Richardson-Burns, M. S.; Sereno, A.; Martin, D. C.; Kotov, H. A. J. Layered Carbon Nanotube-Polyelectrolyte Electrodes Outperform Traditional Neural Interface Materials. *Nano Lett.* **2009**, *9*, 4012–4018.
49. Williams, K. A.; Veenhuizen, P. T. M.; de la Torre, B. G.; Eritja, R.; Dekker, C. Nanotechnology: Carbon Nanotubes with DNA Recognition. *Nature* **2002**, *420*, 761.
50. Hart, A. J.; Boskovic, B. O.; Chuang, A. T. H.; Golovko, V. B.; Robertson, J.; Johnson, B. F. G.; Slocum, A. H. Uniform and Selective CVD Growth of Carbon Nanotubes and Nanofibres on Arbitrarily Microstructured Silicon Surfaces. *Nanotechnology* **2006**, *17*, 1397–1403.
51. Drouvalakis, K. A.; Bangsaruntip, S.; Hueber, W.; Kozar, L. G.; Utz, P. J.; Dai, H. Peptide-Coated Nanotube-Based Biosensor for the Detection of Disease-Specific Autoantibodies in Human Serum. *Biosens. Bioelectron.* **2008**, *23*, 1413–1421.
52. Park, S.; Yang, H.-S.; Kim, D.; Jo, K.; Jon, S. Rational Design of Amphiphilic Polymers to Make Carbon Nanotubes Water-Dispersible, Anti-Biofouling, and Functionalizable. *Chem. Commun.* **2008**, 2876–2878.
53. Curran, S. A.; Ajayan, P. M.; Blau, W. J.; Carroll, D. L.; Coleman, J. N.; Dalton, A. B.; Davey, A. P.; Drury, A.; McCarthy, B.; Maier; *et al*. A Composite from Poly(*m*-phenylenevinylene-*co*-2,5-dioctoxy-*p*-phenylenevinylene) and Carbon Nanotubes: A Novel Material for Molecular Optoelectronics. *Adv. Mater.* **1998**, *10*, 1091–1093.
54. Hellstrom, S. L.; Lee, H. W.; Bao, Z. Polymer-Assisted Direct Deposition of Uniform Carbon Nanotube Bundle Networks for High Performance Transparent Electrodes. *ACS Nano* **2009**, *3*, 1423–1430.
55. Kauffman, D. R.; Star, A. Carbon Nanotube Gas and Vapor Sensor. *Angew. Chem., Int. Ed.* **2008**, *47*, 6550–6570.
56. Lee, H. W.; You, W.; Barman, S.; Hellstrom, S.; LeMieux, M. C.; Oh, J. H.; Liu, S.; Fujiwara, T.; Wang, W. M.; Chen, B.; *et al*. Lyotropic Liquid-Crystalline Solutions of High-Concentration Dispersions of Single-Walled Carbon Nanotubes with Conjugated Polymers. *Small* **2009**, *5*, 1019–1024.
57. Geng, J.; Zeng, T. Influence of Single-Walled Carbon Nanotubes Induced Crystallinity Enhancement and Morphology Change on Polymer Photovoltaic Devices. *J. Am. Chem. Soc.* **2006**, *128*, 16827–16833.
58. Gu, H.; Swager, T. M. Fabrication of Free-Standing, Conductive, and Transparent Carbon Nanotube Films. *Adv. Mater.* **2008**, *20*, 4433–4437.
59. Ago, H.; Petritsch, K.; Shaffer, M. S. P.; Windle, A. H; Friend, R. H. Composites of Carbon Nanotubes and Conjugated Polymers for Photovoltaic Devices. *Adv. Mater.* **1999**, *11*, 1281–1285.
60. Star, A.; Stoddart, J. F.; Steuerman, D.; Diehl, M.; Boukai, A.; Wong, E. W.; Yang, X.; Chung, S.-W.; Choi, H.; Heath, J. R. Preparation and Properties of Polymer-Wrapped Single-Walled Carbon Nanotubes. *Angew. Chem., Int. Ed.* **2001**, *40*, 1721–1725.
61. Kimura, M.; Miki, N.; Adachi, N.; Tatewaki, Y.; Ohtaa, K.; Shiraiab, H. Organization of Single-Walled Carbon Nanotubes Wrapped with Liquid-Crystalline π-Conjugated Oligomers. *J. Mater. Chem.* **2009**, *19*, 1086–1092.
62. Chen, J.; Liu, H.; Weimer, W. A.; Halls, M. D.; Waldeck, D. H.; Walker., G. C. Noncovalent Engineering of Carbon Nanotube

Surfaces by Rigid, Functional Conjugated Polymers. *J. Am. Chem. Soc.* **2002**, *124*, 9034–9035.
63. Chen, J.; Ramasubramaniam, R.; Xue, C.; Liu, H. A New Method for the Preparation of Stable Carbon Nanotube Organogels. *Adv. Funct. Mater.* **2006**, *16*, 114–119.
64. Zou, J.; Khondaker, S. I.; Huo, Q.; Zhai, L. A General Strategy to Disperse and Functionalize Carbon Nanotubes Using Conjugated Block Copolymers. *Adv. Funct. Mater.* **2009**, *19*, 479–483.
65. Satishkumar, B. C.; Brown, L. O.; Gao, Y.; Wang, C.-C.; Wang, H.-L.; Doorn, S. K. Reversible Fluorescence Quenching in Carbon Nanotubes for Biomolecular Sensing. *Nat. Nanotechnol.* **2007**, *2*, 560–564.
66. Kang, Y. K.; Lee, O.-S.; Deria, P.; Kim, S. H.; Park, T.-H.; Bonnell, D. A.; Saven, J. G.; Therien, M. J. Helical Wrapping of Single-Walled Carbon Nanotubes by Water Soluble Poly(*p*-phenyleneethynylene). *Nano Lett.* **2009**, *9*, 1414–1418.
67. Casagrande, T.; Imin, P.; Cheng, F.; Botton, G. A.; Zhitomirsky, I.; Adronov, A. Synthesis and Electrophoretic Deposition of Single-walled Carbon Nanotube Complexes with a Conjugated Polyelectrolyte. *Chem. Mater.* **2010**, *22*, 2741–2749.
68. Baykal, B.; Ibrahimova, V.; Er, G.; Bengu, E.; Tuncel, D. Dispersion of Multi-Walled Carbon Nanotubes in an Aqueous Medium by Water-Dispersible Conjugated Polymer Nanoparticles. *Chem. Commun.* **2010**, *46*, 6762–6764.
69. Deria, P.; Sinks, L. E.; Park, T. H.; Tomezsko, D. M.; Brukman, M. J.; Bonnel, D. A.; Therien, M. J. Phase Transfer Catalysts Drive Diverse Organic Solvent Solubility of Single-Walled Carbon Nanotubes Helically Wrapped by Ionic, Semiconducting Polymers. *Nano Lett.* **2010**, *10*, 4192−4199.
70. Nish, A.; Hwang, J.-Y.; Doig, J.; Nicholas, R. J. Highly Selective Dispersion of Single-Walled Carbon Nanotubes Using Aromatic Polymers. *Nat. Nanotechnol.* **2007**, *2*, 640–646.
71. Singh, P.; Toma, F. M.; Kumar, J.; Venjatesh, V.; Raya, J.; Prato, M.; Febre, B.; Verma, S.; Bianco, A. Carbon Nanotube-Nucleobase Hybrids: Nanorings from Uracil-Modified Single-Walled Carbon Nanotubes. *Chem. Eur. J.* **2011**, *17*, 6772–6780.
72. Singh., P.; Kumar, J.; Toma, F. M.; Raya, J.; Prato, M.; Febre, B.; Verma, S.; Bianco, A. Synthesis and Characterization of Nucleobase-Carbon Nanotube Hybrids. *J. Am. Chem. Soc.* **2009**, *131*, 13555–13562.
73. Sarikaya, M. C.; Temerler, K. Y.; Jen, K.; Shulten; Baneyx, F. Molecular Biomimetics: Nanotechnology Through Biology. *Nat. Mater.* **2003**, *2*, 577–585.
74. Quintana, M.; Prato, M. Supramolecular Aggregation of Functionalized Carbon Nanotubes. *Chem. Commun.* **2009**, 6005–6007.
75. Price, B. K.; Tour, J. M. Functionalization of Single-Walled Carbon Nanotubes "On Water". *J. Am. Chem. Soc.* **2006**, *128*, 12899–12904.
76. Wu, W.; Wieckowsk, S.; Pastorin, G.; Benincasa, M.; Klumpp, C.; Briand, J.-P.; Gennaro, R.; Prato, M.; Bianco, A. Targeted Delivery of amphotericin B to Cells by Using Functionalized Carbon Nanotubes. *Angew. Chem., Int. Ed.* **2005**, *44*, 6338–6362.
77. Piot, L.; Palma, C.-A.; Llanes-Pallas, A.; Prato, M.; Szekrényes, Z.; Kamarás, K.; Bonifazi, D.; Samorì, P. Selective Formation of Bi-Component Arrays Through H-Bonding of Multivalent Molecular Modules. *Adv. Funct. Mater.* **2009**, *19*, 1207–1214.
78. Brienne, M.-J.; Gabard, J.; Lehn, J.-M.; Stibor, I. Hydrogen-Bonding Interactions in the Series of Complexes $[M(C_4O_4)(OH_2)_2(dmf)_2]$ and $[M(C_4O_4)(OH_2)_4]$ (M = Mn, Co, Ni, Cu, Zn). *J. Chem. Soc., Chem. Commun.* **1989**, 1868–1970.
79. Kotera, M.; Lehn, J.-M.; Vigneron, J. P. Self-Assembled Supramolecular Rigid Rods. *J. Chem. Soc., Chem. Commun.* **1994**, 197–199.
80. Brunsveld, L.; Folmer, B. J. B.; Meijer, E. W.; Sijbesma, R. P. Supramolecular Polymers. *Chem. Rev.* **2001**, *101*, 4071–4097.
81. http://www.nanocyl.com/en/Products-Solutions/Products/Nanocyl-NC-7000-Thin-Multiwall-Carbon-Nanotubes.
82. Yan, M.; Harnish, B. A Simple Method for the Attachment of Polymer Films on Solid Substrates. *Adv. Mater.* **2003**, *15*, 244–248.
83. Cellot, G.; Cilia, E.; Cipollone, S.; Rancic, V.; Sucapane, A.; Giordani, S.; Gambazzi, L.; Markram, H.; Grandolfo, M.; Sacaini, D.; *et al*. Carbon Nanotubes Might Improve Neuronal Performance by Favouring Electrical Shortcuts. *Nat. Nanotechnol.* **2009**, *4*, 126–133.